SUMMARY OF AERODYNAMIC VIBRATION EFFECTS ON A.L.L. TURRET

P. MERRITT

L. SHER

Air Force Weapons Laboratory, Kirtland AFB NM

The use of a laser system in an aircraft requires an understanding of the effects of the airborne environment on the laser system. The time averaged intensity of the laser at the target will be reduced if the optical elements of the system are caused to be jittered. The airborne environment provides sources of angular and linear vibrations that cause laser beam jitter. These vibrations can come fom the vehicle itself or, if the optical elements are exposed or vented to the airstream, this can provide a direct torque disturbance on the optical elements. Figure 1 schematically depicts these two main sources of jitter. In the upper figure, the optical element is shown on bearings which give it two degrees of freedom. The mirror would actually be surrounded by a telescope housing which would be rotated to point the beam. When the use of a window is precluded, such as for very high power, the external airstream provides a direct torque excitation to the mirror. In general, for a arbitrary pressure distribution, the torques on the mirror would be

$$M_x(t) = -\iint_A y \; p(x,y,t)\,dxdy$$

$$M_y(t) = \iint_A x \; p(x,y,t)\,dxdy$$

If the pressures were constant in space over halves of the mirror, e.g.,

$$p(x,y,t) = p_1(t) \qquad y>0$$

$$p(x,y,t) = p_2(t) \qquad y<0$$

then

$$M_x(t) = 0.08\ D^3\ [p_2(t) - p_1(t)]$$

$$M_y(t) = 0$$

where D is the mirror diameter. The torque is seen to scale with diameter cubed. Given the power and cross spectra of the pressures then the power spectrum of the torque would be

$$\Phi_{Mx}(f) = (.08D^3)^2\ [\Phi_{p_1} + \Phi_{p_2} - 2Re\psi_{p_1p_2}]$$

where Φ denotes a power spectrum and ψ denotes a cross spectrum. For p_1 and p_2 equal but uncorrelated, or perhaps correlated 180° out of phase, one sees that a torque will still result.

The optical system is pointed at the target by using some type of optical tracking system. However the primary mirror, the one disturbed by the pressure fluctuations, is inertially stabilized by using gyroscopes attached to the back of the mirror. A simplified schematic of such a system is shown in Figure 2. If the transfer function from torque, T_q to mirror motion, ε, is calculated it is found to be;

$$(\varepsilon/T_q) = (1/J_m)/(s^2 + K_T/J_m)$$

This transfer function is a constant, $1/K_T$, for low frequencies, and reduces at 40 dB per decade above the corner frequency K_T/J_m. This indicates that the system only rejects low frequencies by the strength of its torquer.

Higher frequency torques are rejected by the inertia of the primary mirror and its structure. The closed loop bandwidth, K_T/J, is typically 100 Hz, therefore the response of the telescope mirror to direct torques may be considered as two frequency regions, from d.c. to K_T/J, and from K_T/J to infinity. The following equations permit us to consider the previous developed PSD expressions based on pressure, to evaluate the mean square error,

$$\bar{\varepsilon}^2 = \int_0^{K_T/J} (\Phi_M K_T^2)\,d\omega \quad \text{for } 2\pi f < K_T/J$$

$$\bar{\varepsilon}^2 = \int_{K_T/J}^{\infty} (\Phi_M/J^2\omega^4)\,d\omega \quad \text{for } 2\pi f > K_T/J$$

The other effect of the flow is the motions of the turret induced by the steady and fluctuating pressure. The motion of the turret can be coupled to the optical elements by several mechanisms which are shown in Figure 3. The motion of the turret in response to the aerodynamically generated torques, T_t, are determined by the inertia of the turret, J_t, and its mounting compliance, K. A mechanical transfer function from torque to angular motion, θ, results in a transfer function of the same form as developed for the mirror motion. Therefore, at low frequencies the motion of the turret is $(\theta/T_t) = (1/K)$

At high frequencies

$$(\theta/T_t) = (1/J\omega^2)$$

The first flights of the Airborne Laser Laboratory (ALL) in the Cycle I test program gave an indication that the optical jitter, ε, varied with the flight dynamic pressure, q_∞, see e.g. Figure 4. Since the net pressure difference either across the mirror or across the turret is the quantity of interest it makes sense that the torque, and thus the jitter will scale with q_∞. Theoretically it, probably makes more sense to use the difference between stagnation pressure P° and static pressure P_∞ as the dependent variable, i.e.,

$$p^\circ - p_\infty = [(p^\circ/p_\infty)-1]\ p_\infty$$

The function p°/p_∞ is a complicated function of Mach number and specific heat. For $M<0.6$, one can approximate the above to within 10% by

$$p^\circ - p_\infty = q_\infty = \tfrac{1}{2}\ \rho_\infty\ V_\infty^2$$

Early tests of a dummy turret with a cavity on a KC-135 in which fluctuating pressures were measured, Reference 1, indicated numerous acoustic resonances and torque levels approaching 2000 inch lbs on the exposed mirror. A comprehensive test series in wind tunnels, reference 2, led to dramatic reductions in the levels of fluctuating torques on the mirror to the order of 50 in lbs by the addition of external fences on the Advanced Pointing and Tracking. In addition, the acoustic resonances were reduced in intensity. In the next flight program of the Airborne Laser Laboratory, Cycle II, the actual pointing and tracking telescope was instrumented with pressure transducers, see Figure 5, which were differenced and suitably scaled for telescope area and moment arm to indicate torque. The results are shown in Figure 6, where the torque spectrum for wind tunnel results and for the airborne measurements are shown. The torque spectra have been normalized by

$$L^6 M^4 P^2 / S$$

Where L - Aperture diameter

M - Mach Number

P - free stream pressure

and

$S = V/L$

Where V - free stream velocity.

The wind tunnel data shown in Figure 6 was obtained using the on gimbal telescope model used for the Large Pointing System test series. An attempt was also made to use the 0.3 scale APT model test results, however poor correlation was obtained. It was discovered that the APT model was not vented internally and thus did not match the actual airborne telescope which is vented to the turret.

The magnitude of the torque measured for the modified flight turret was insignificant in terms of the jitter generated. An attempt to correlate a pressure measurement in the cavity with the jitter of the telescope is shown in Figure 7. Just observing the pressure spectrum and the jitter spectrum, one might be tempted to infer that the pressure spectrum is driving the jitter. However, the coherence spectrum shown at the center shows correlation only at several high frequency spikes. The coherent power between pressure and jitter indicated only about 3 percent of the jitter was correlated with pressure fluctuations. Follow-on tests with a window installed over the cavity yielded essentially the same telescope jitter as the open cavity again verifying the direct aerodynamics torques on the mirror were insignificant.

The Cycle II test series conducted numerous tests to explore the potential variables that influence system jitter. Based on the measurements of fluctuating pressures in the cavity, it was concluded that the vibration of the turret was the main source of jitter excitation. Attempts to correlate jitter with dynamic pressure are shown in Figure 8, which shows a large spread in the data. However by restricting several variables, the correlation of jitter with dynamic pressure, in particular the circled data points, was much more obvious. However a lack of angular instrumentation made it impossible to acquire data during Cycle II to accurately correlate turret vibration with flight parameters such as dynamic pressure and Mach number.

Prior to Cycle III flight testing the Air Force acquired some precision angular displacement transducers to install on the turret. These transducers along with several pressure transducers were installed on a dummy turret in the initial flight tests of the ALL for Cycle III. Further, it was possible to define a series of tests where one flight parameter was varied while holding others fixed. In particular, a series of tests were run where q_∞ was held constant and Mach number changed, and a similar series where the Mach number was held constant and the q_∞ was changed.

The flight tests have yielded some interesting and unexpected results. Figure 9, shows the effect on roll angular vibration when changing q_∞ with Mach held constant. The data indicates that the vibration does change linearly with q_∞ but it also shows a distinct dependency on Mach number. The higher Mach number shows considerably less vibration. The effect is further amplified by referring to Figure 10 which shows the effect of

changing Mach number while holding a constant dynamic pressure. The data shows a nonlinear decrease in vibration with increasing Mach number. The spike in Figure 10 labeled "Shudder experiment" is another interesting aspect of the vibration. The ALL crew had described a strong vibration effect at .51 Mach number. In the data of Figure 10 labeled Mission 5 the pilot attempted to "feel out" the high vibration point and hold it for several seconds. The plotted spike in the data confirms the aircraft "Shudder Area".

It was also possible to analyze the flight test data for frequency content. This data is shown in Figures 11 and 12. The effect of changing q_∞ while holding Mach number constant appears to change the entire level of the PSD with little effect on the frequency content. This is shown as Figure 11. However, when the Mach number was lowered, a distinct increase in low frequency vibration, below 20 Hz was obvious, see Figure 12. The low Mach numbers must change the flow pattern over the turret in such a way that the airflow imparts a much stronger driving torque to the APT turret.

Pressure measurements on the external pressures at 4 points on the dummy turret were taken concurrent with the vibration data. Figure 13 is included to show the pressure from a transducer labeled R103 which was at the vertical center of the turret and 50 degrees CCW from the leading edge and transducer R104 which was at vertical center and aft. It is interesting to see that the pressure measurements follow the same trend as the vibration measurements. Notice that the 50° transducer shows more variation the PSD at various Mach numbers, but the aft transducer contains considerable more energy in the PSD. The RMS level plots of the transducers were

similar in shape to the angular vibration shown in Figure 10.

The data now available well documents the base motion response of the turret to air loads during flight. This data can be used to select flight conditions for this aircraft that will yield low base motion. However the data does not provide an understanding of the physics of the aerodynamic phenomena. If the vibration is to be reduced by using different fairings or if this data is to be used to design a future turret, the physical basis of the airflow needs to be understood. Since this paper has pointed out that turret base motion is the major driving source for jitter, it would be most beneficial to pursue this analytical area. Probably wind tunnel tests are not the correct approach since the problem requires convolving structural design of the turret with aerodynamic loading. However, a large amount of flight data is available, including pressures, angular, and linear vibration data.

In conclusion, this paper has summarized the effects of the airborne environment on a pointing and tracking system using a turret external to an aircraft. The data has covered a series of flight tests and a span of seven years. The two major airborne effects were shown to be direct pressure loading of optical elements and vibrations of the entire turret. The direct optical loading problem has been minimized by clever fence designs for the turret, however the turret vibration problem is a poorly understood area. A large amount of data has recently been obtained to document the turret vibration but a physical understanding of the problem is yet to be attempted.

REFERENCES

1. "Estimation of Steady and Unsteady Torques Acting on a Large Cavity Fairing into the Airstream," GD Convair Div, Fort Worth, TX, Report No. F2A-453, September 1971.

2. Van Kuren, James T., et al, "Acoustic Phenomena of Open Cavity Airborne Cassegrainian Telescopes", AIAA paper No. 74-196, AIAA 12th Aerospace Science Meeting, Jan 30, 1974.

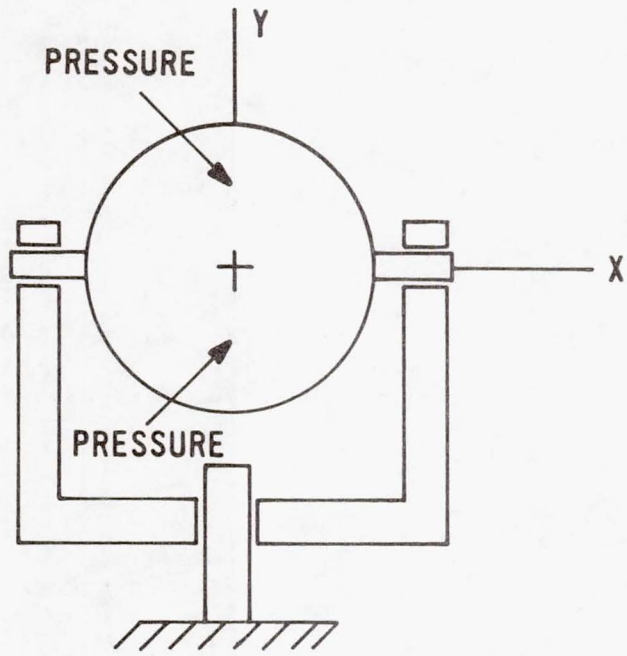

DIRECT LOADING OF OPTICAL ELEMENT

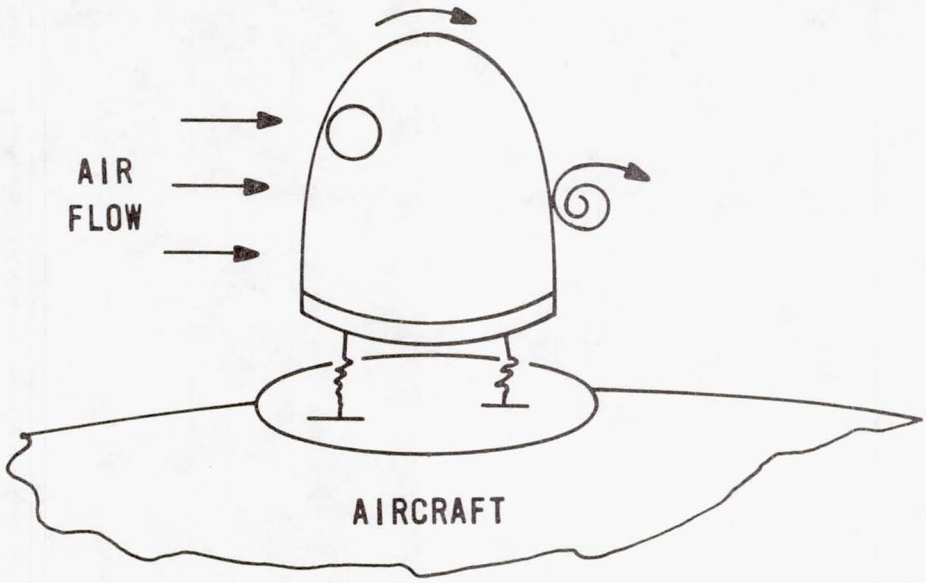

FLOW INDUCED TURRET VIBRATION

Figure 1. Sources of Aerodynamic Jitter.

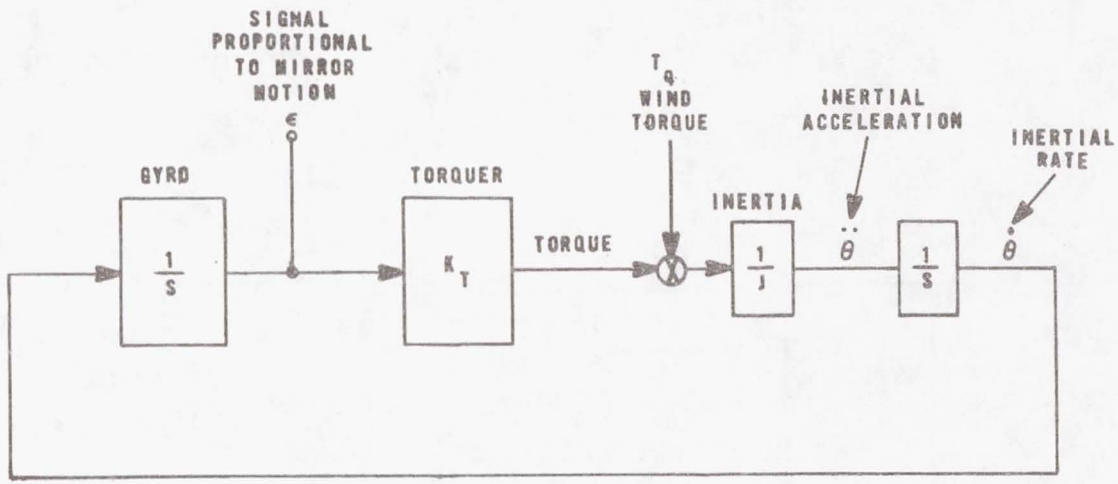

Figure 2. Servosystem Diagram for Gyro Stabilized Pointing Mirror.

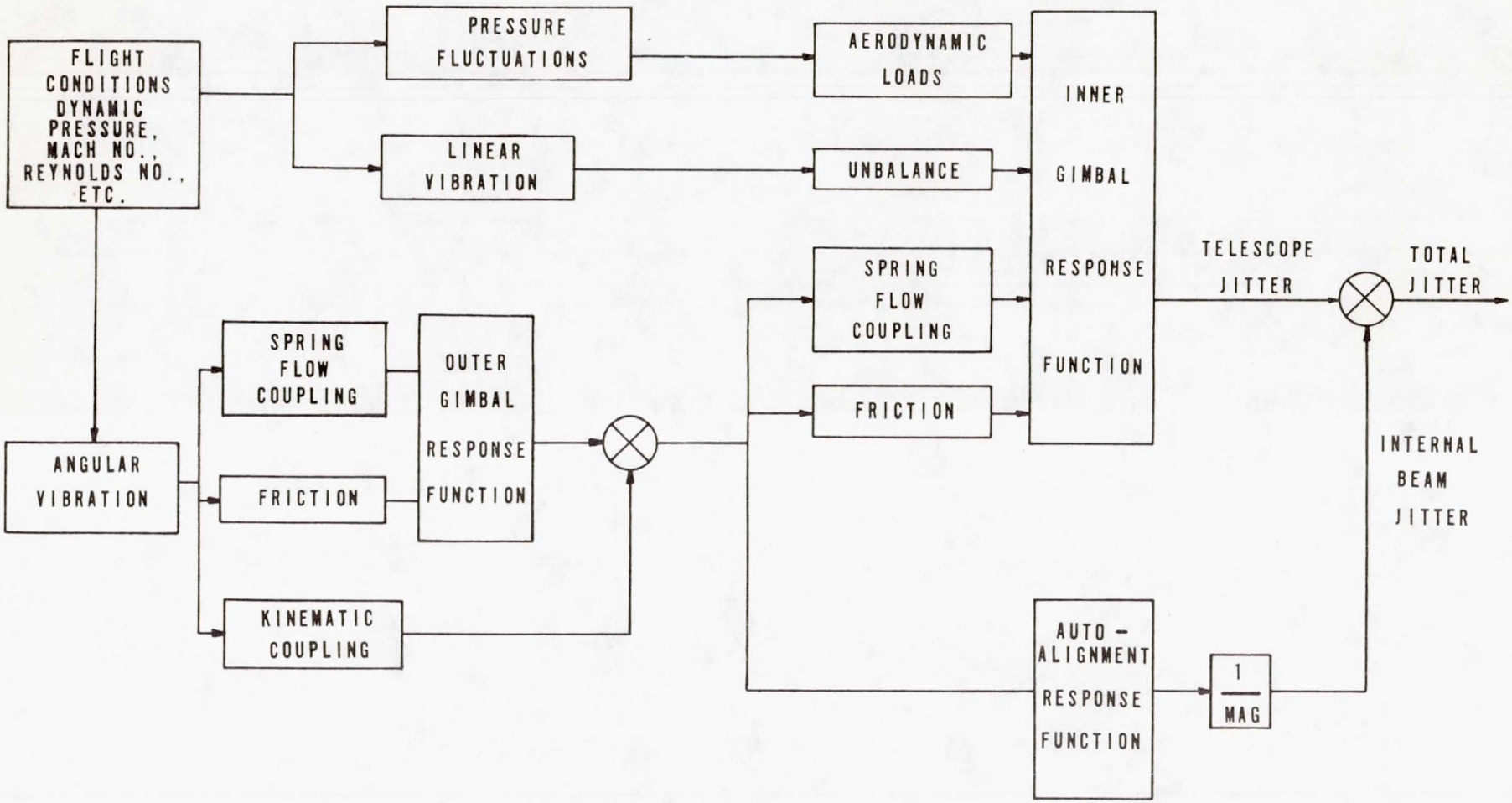

Figure 3. Coupling Paths Between Vibration and Beam Jitter.

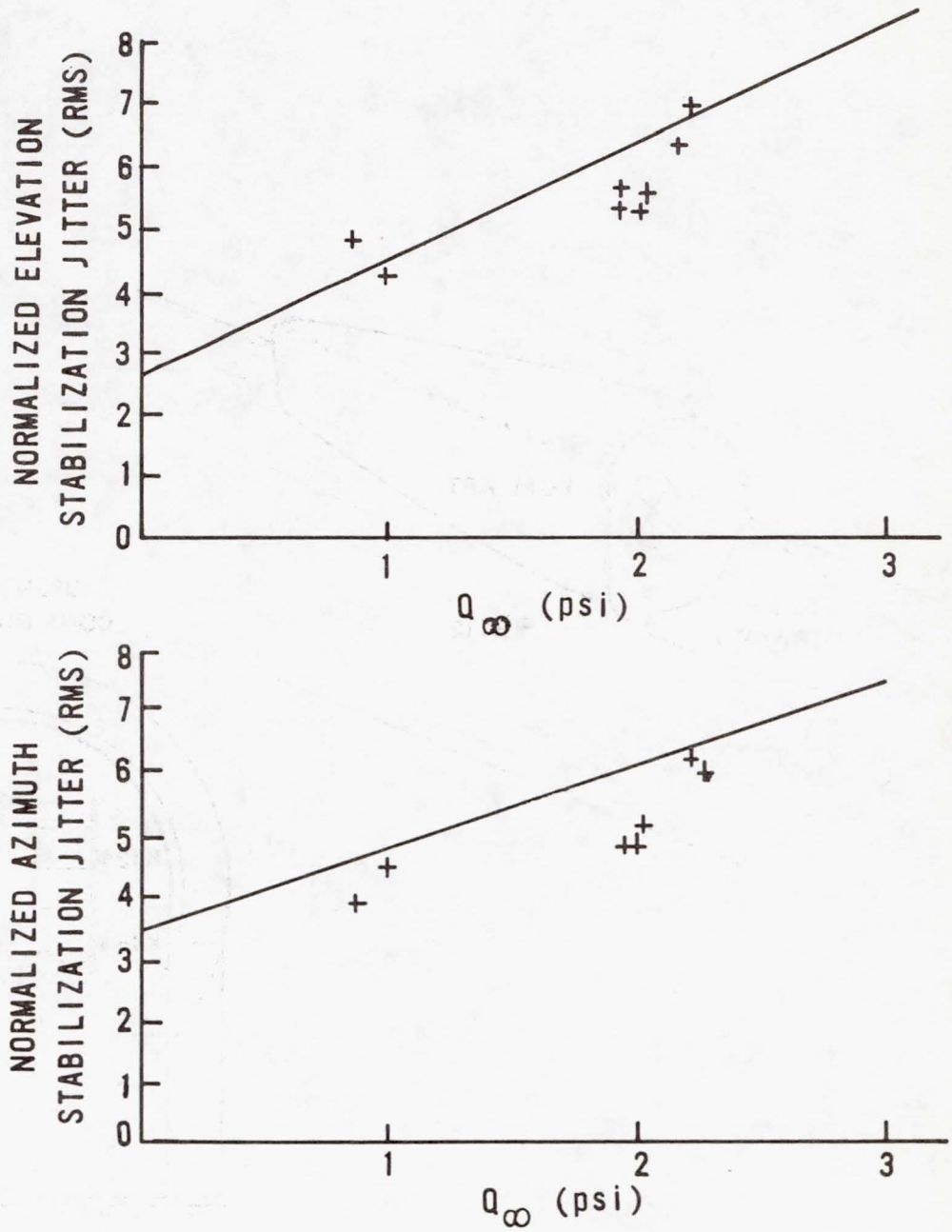

Figure 4. Stabilization Jitter from Cycle I Versus Dynamic Pressure.

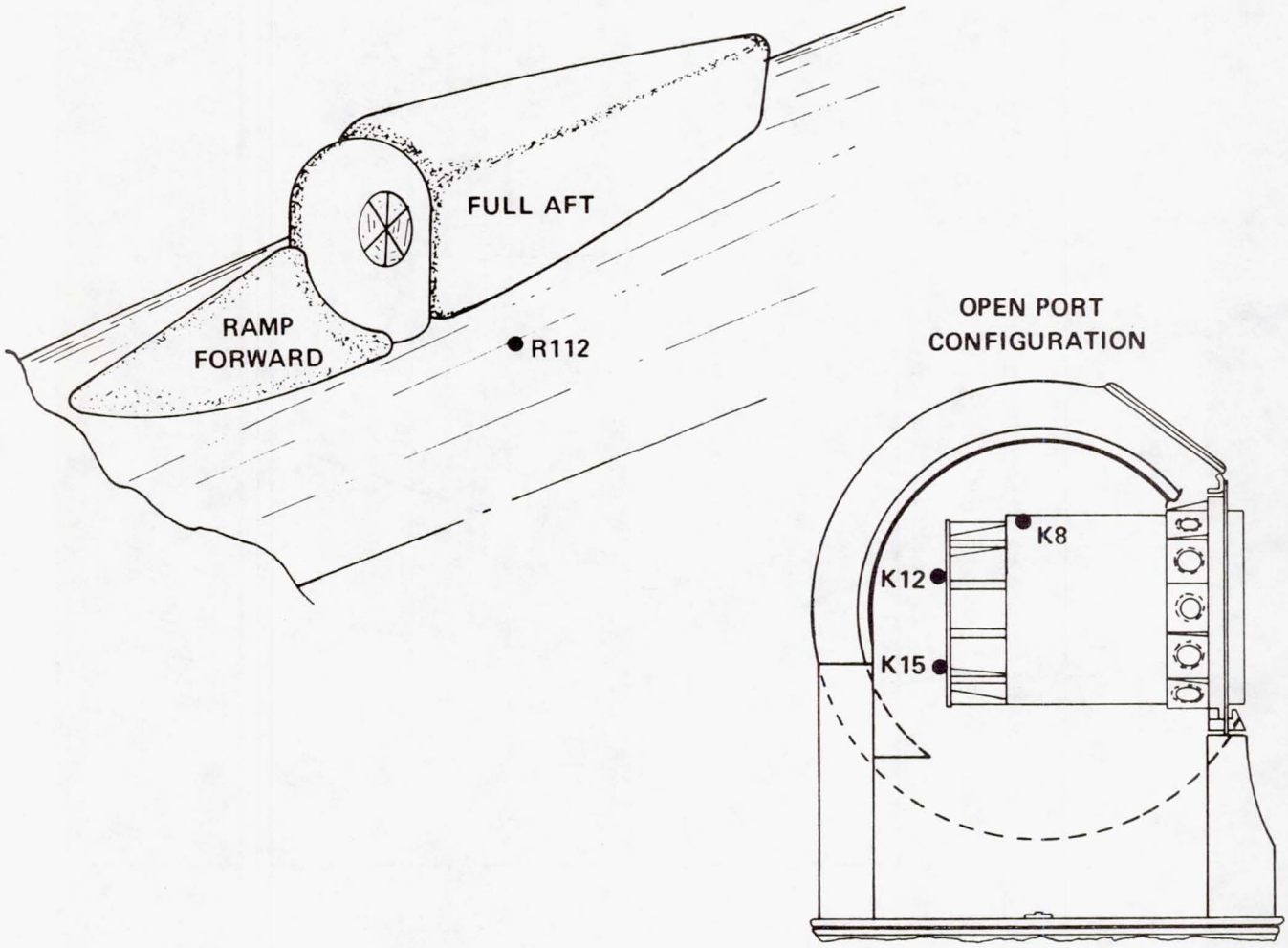

Figure 5. Location of Pressure Transducers for Cycle II Flight Tests.

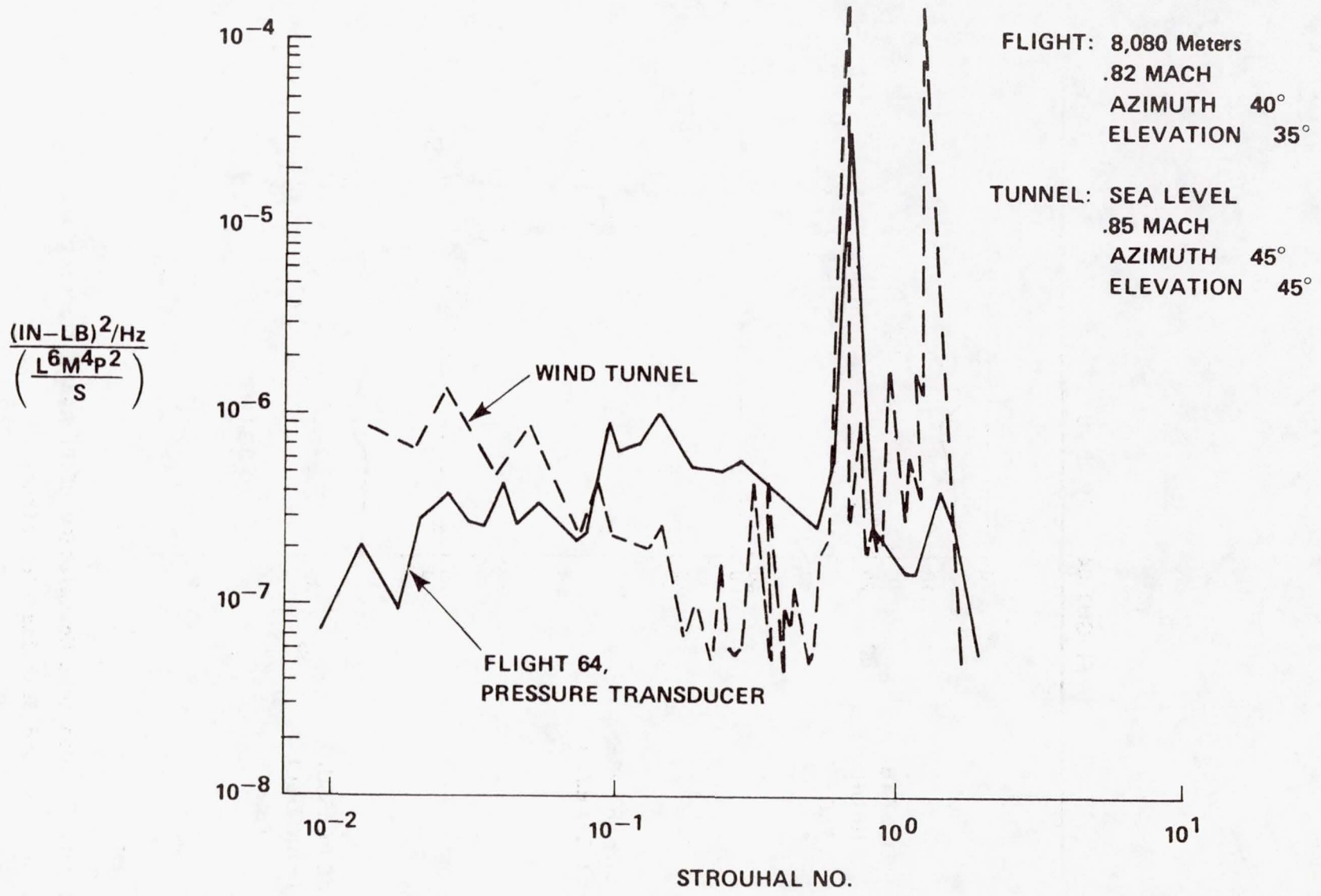

Figure 6. Correlation of Wind Tunnel and Flight Test Torques.

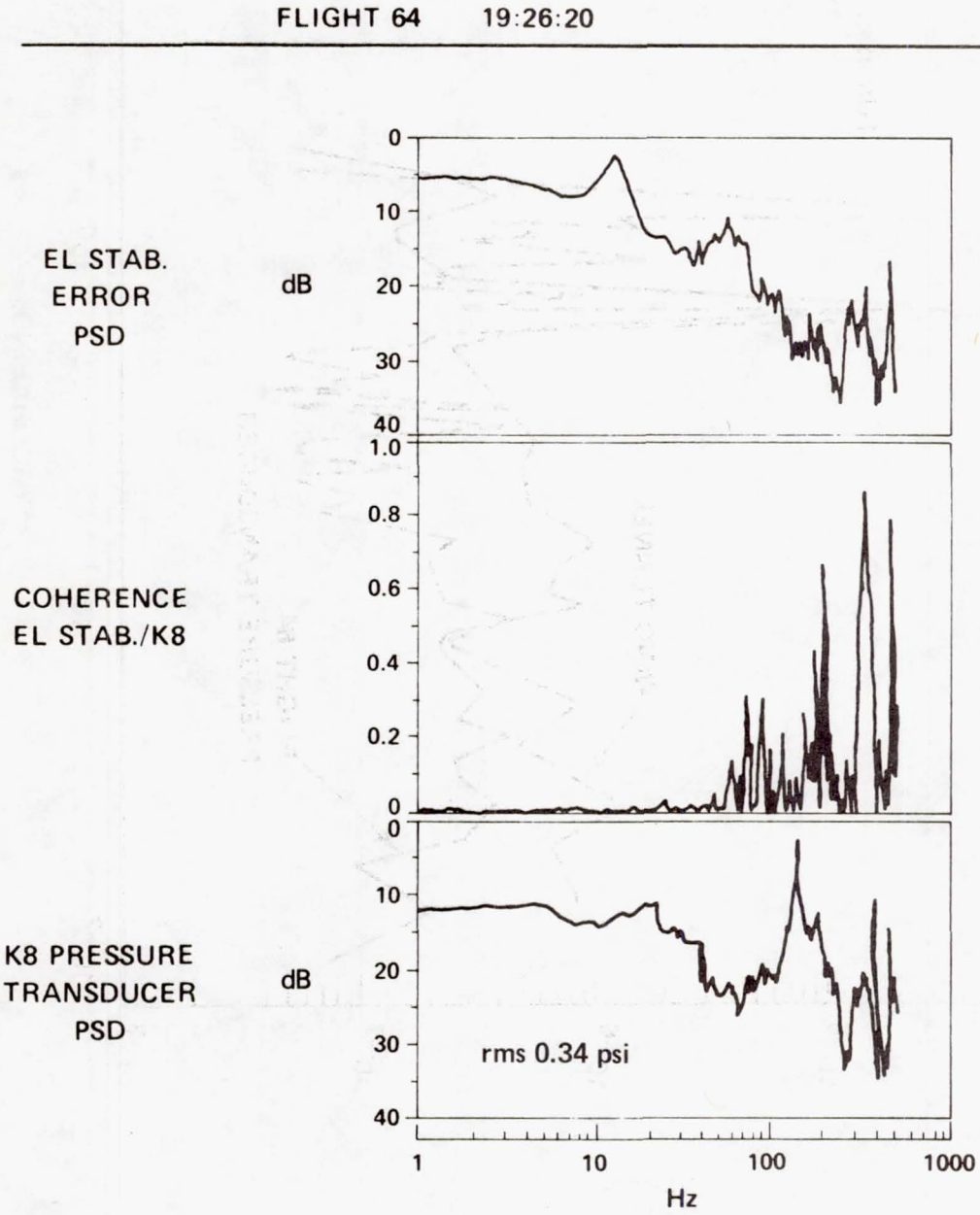

Figure 7. Coherent Correlation of Pressure Fluctuations and Stabilization Jitter.

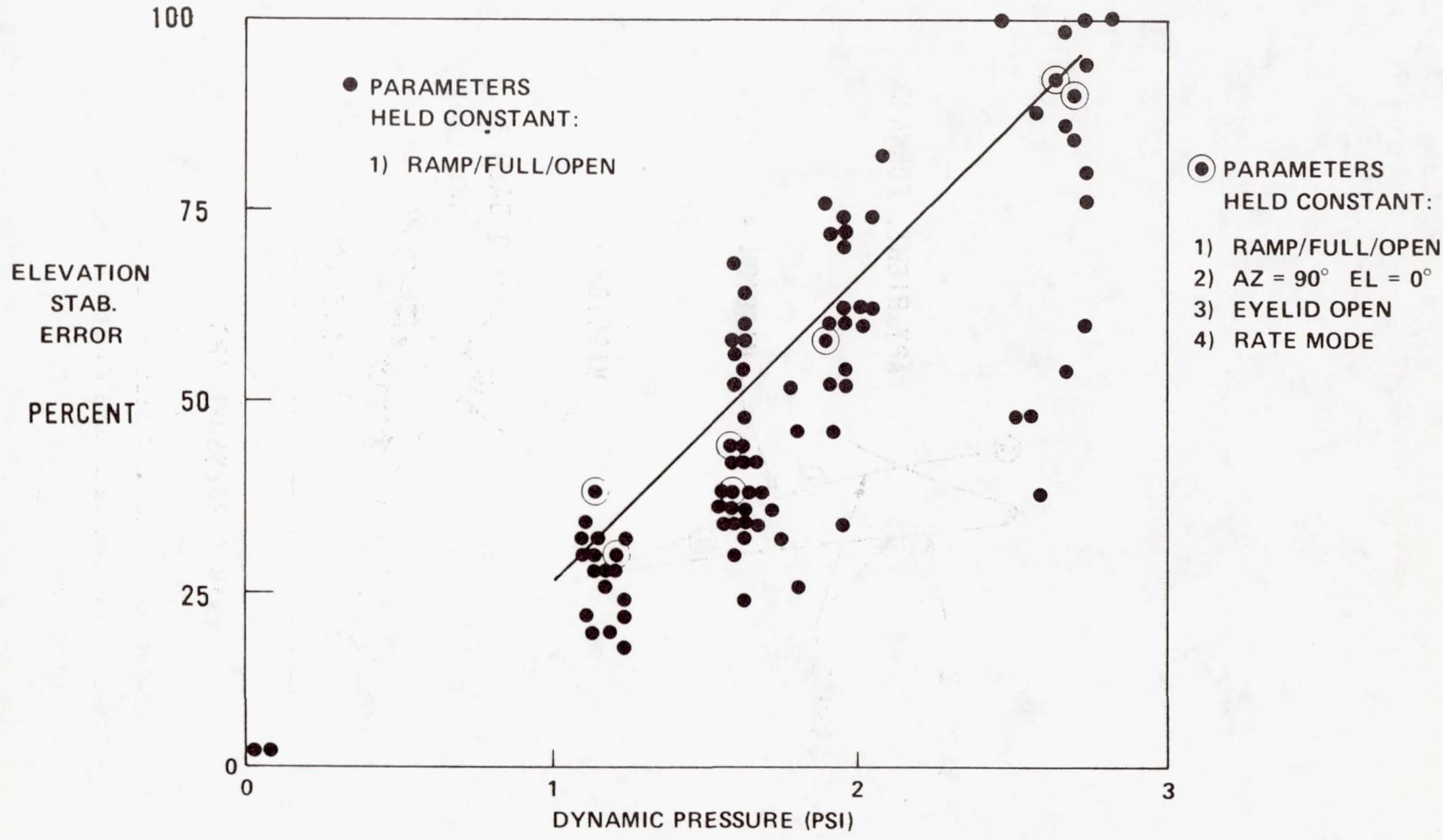

Figure 8. Correlation of Cycle II Stabilization Jitter With Dynamic Pressure.

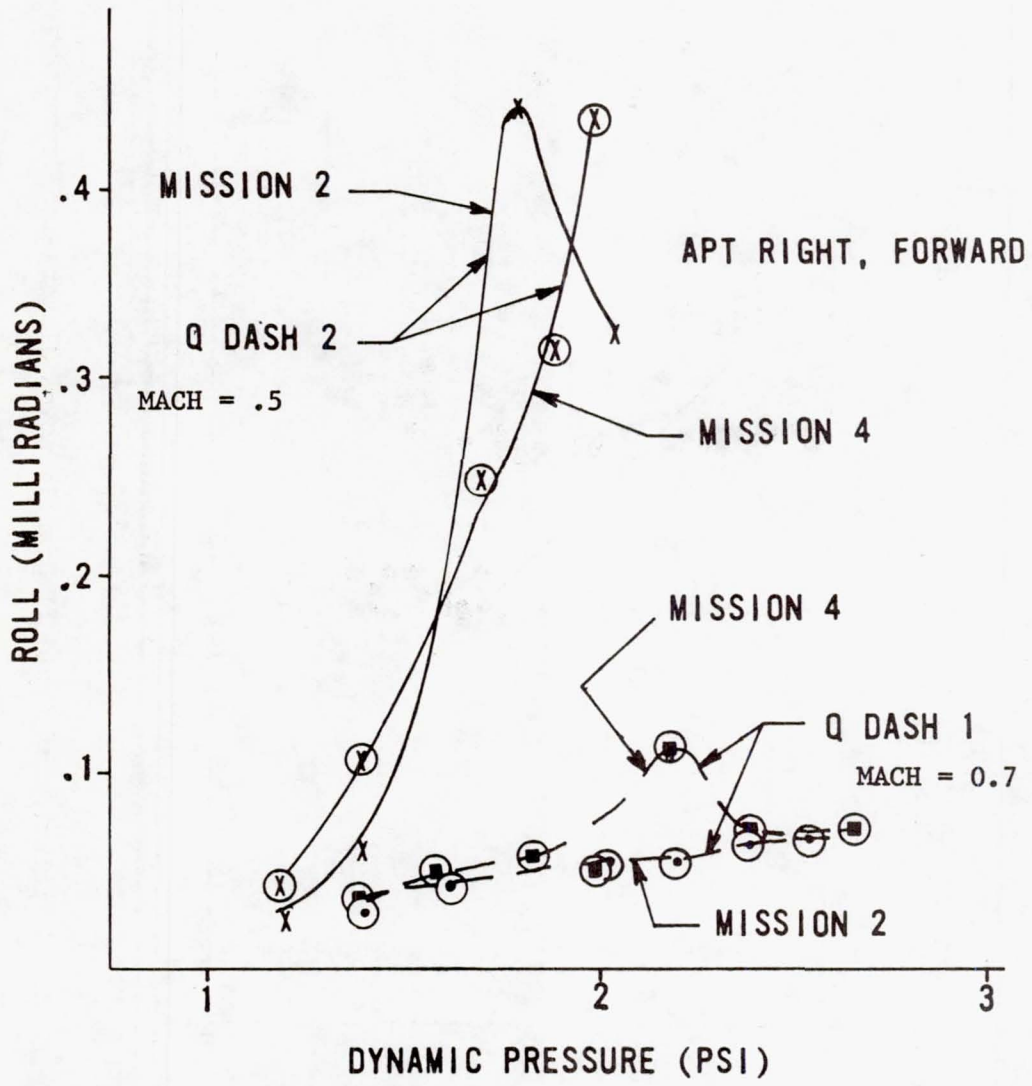

Figure 9. Correlation of Turret Vibration With Dynamic Pressure for Constant Mach Number (Vibration levels are rms).

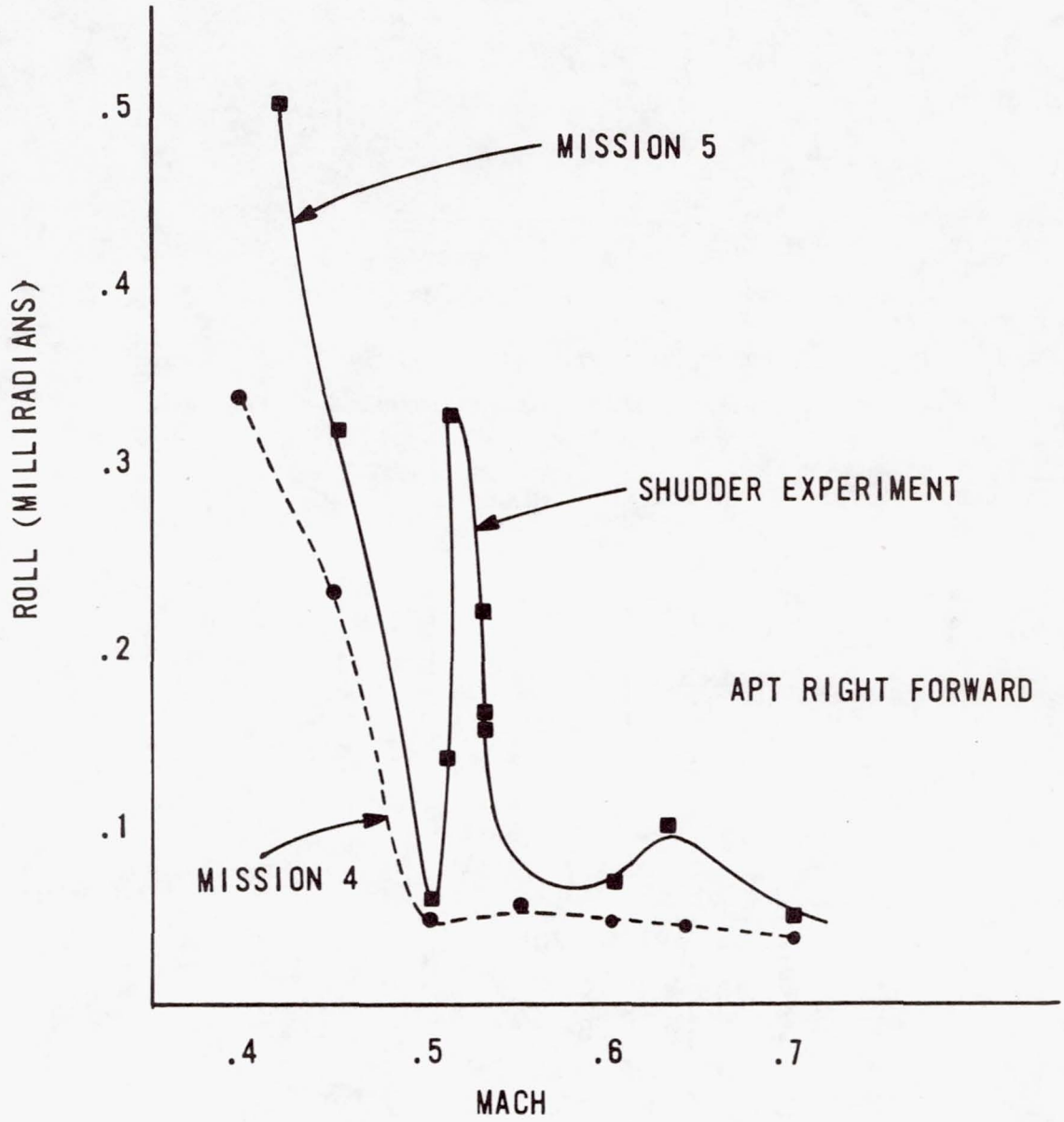

Figure 10. **Correlation of Turret Vibration With Mach Number, Dynamic Pressure Constant at 1.25 psi** (Vibration levels are rms).

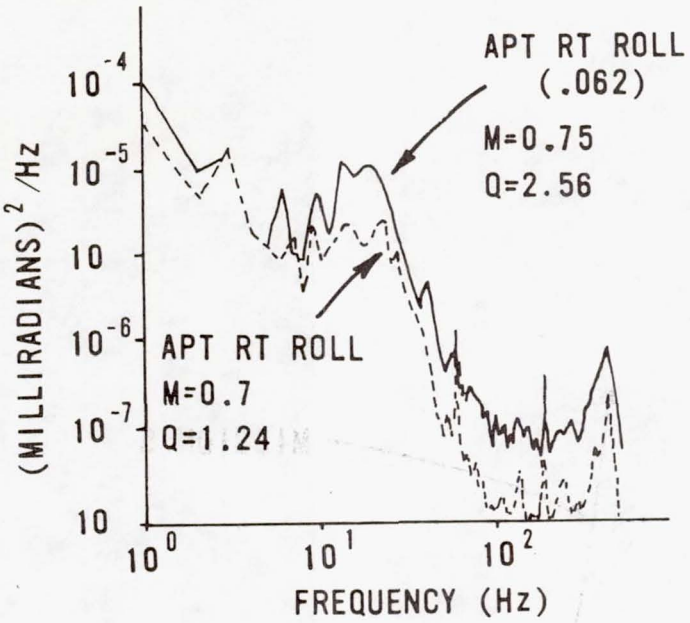

Figure 11. PSD's of Turret Vibration for Two Different Dynamic Pressures, Constant Mach.

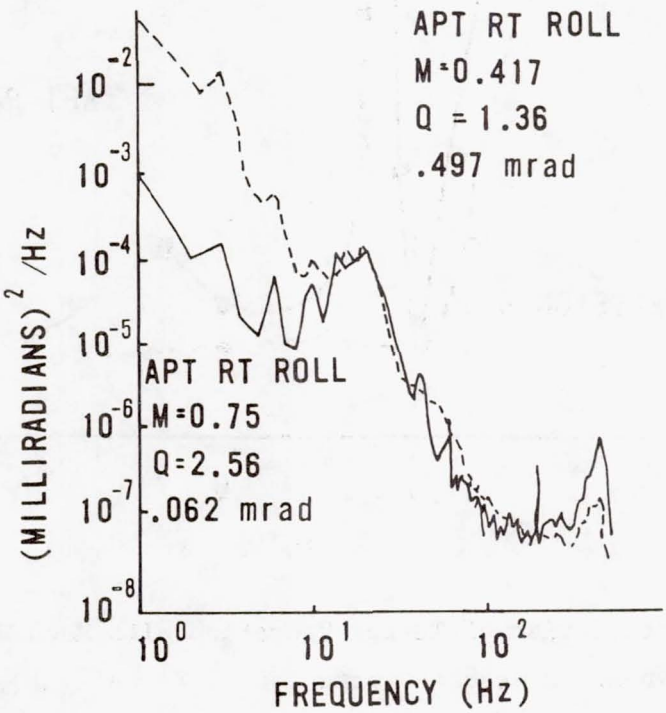

Figure 12. PSD's of Turret Vibration for Changes in Mach Number and Dynamic Pressure.

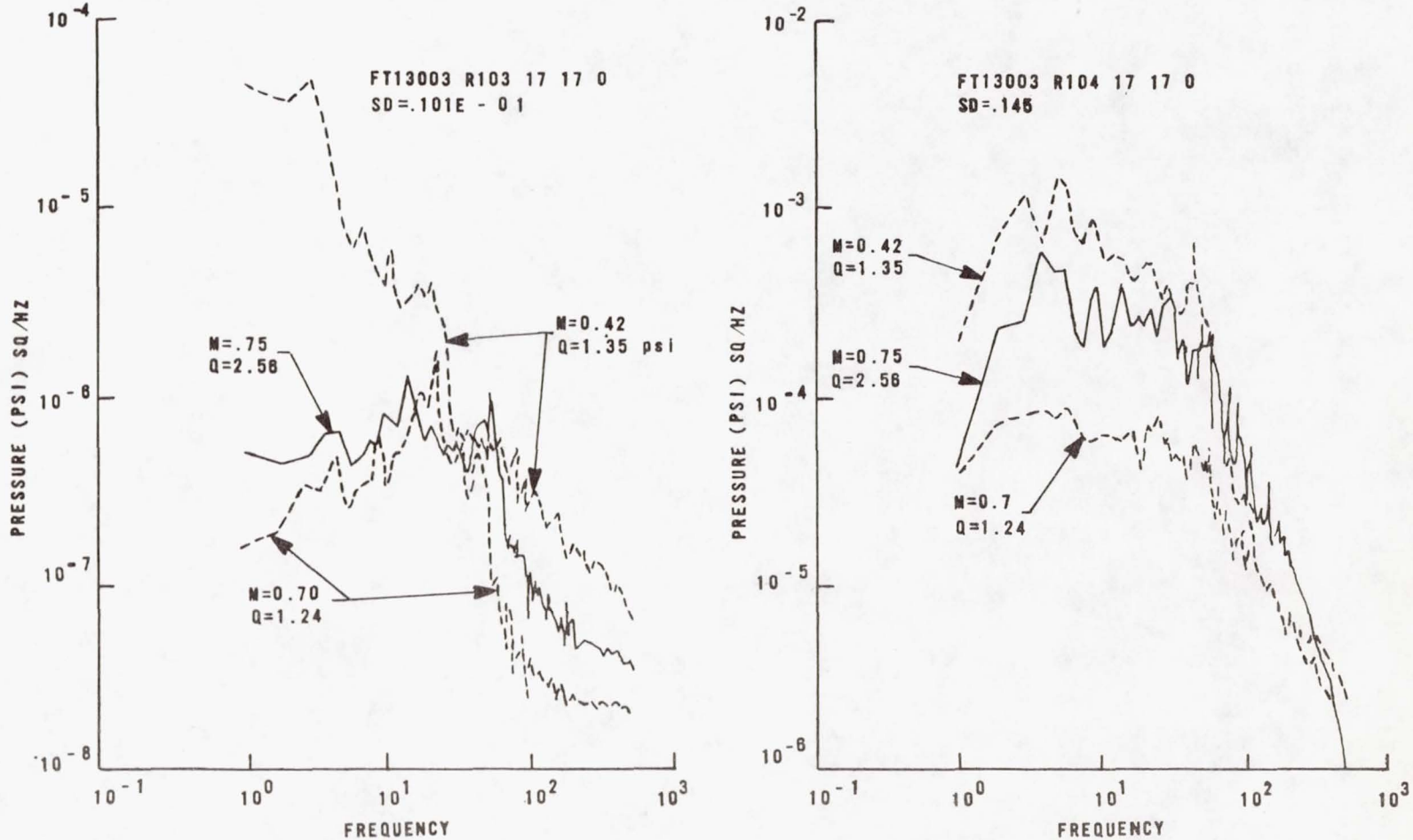

Figure 13. PSD Analyses of Pressure Transducers on Exterior Surface of Dummy Turret.